INTERNATIONAL JOURNAL OF ELECTRICAL ENGINEERING & TECHNOLOGY (IJEET)

ISSN 0976 – 6545(Print)
ISSN 0976 – 6553(Online)
Volume 3, Issue 1, January- June (2012), pp. 100-111
© IAEME: www.iaeme.com/ijeet.html
Journal Impact Factor (2011): 0.9230 (Calculated by GISI)
www.jifactor.com

IJEET
©IAEME

ROGOWSKI COIL EVALUATION PERFORMANCE WITH DIFFERENT FAULT CONDITIONS IN MEDIUM VOLTAGE DISTRIBUTION NETWORKS

[*#]Muzamir Isa, *Matti Lehtonen
*Department of Electrical Engineering, Aalto University, School of Science and Technology,
Otakaari 5 I, Espoo, PO Box 13000, FI-00076 Aalto, Finland
[#]School of Electrical Systems Engineering, Universiti Malaysia Perlis, Malaysia
Email: muzamirisa@gmail.com, Fax: +358 9 451 5012

Ghulam M. Hashmi
Department of Energy Sytems, VTT Technical Research Centre of Finland, P. O. Box 1000, FIN-02044, Espoo, Finland

Nagy I. Elkalashy
Department of Electrical Engineering, Shebin Elkom, Minoufiya University, Egypt

ABSTRACT

In this paper, Electromagnetic Transient Program-Alternative Transient Program (EMTP-ATP) test bench of 20 kV network is developed considering high frequency models of Rogowski coil and the distribution network. The bench test is used to evaluate the Rogowski performance with different fault scenarios such as different fault types, different fault resistances and inception angles. Furthermore, the tree leaning fault and arcing fault with characteristics of intermittent faults are considered in the study. Results show the possibility of using Rogowski coil for locating faults in the medium voltage (MV) distribution networks.

Keywords: Rogowski coil, Medium Voltage networks, Intermittent and high impedance arcing faults.

1 INTRODUCTION

In 1912, the Rogowski coil was introduced to measure the magnetic fields. Since the coil output voltage and power were not sufficient enough to drive measuring equipments, it has been widely used for measuring fast, high-level pulsed currents in the range of a few mega-amperes rather than in power system [1]. With the improvement of today's microprocessor-based protection relays and measurement devices, the Rogowski coils become more suitable for those applications. They have generally been used where other devices cannot help [2]. They have become an increasingly popular method of measuring current within power electronics equipment due to their advantages of low insertion loss and reduced size as compared to an equivalent CT [3]. They are preferred method of current measurements having more suitable features than CTs and other iron-cored devices. The features of the Rogowski coils which make them particularly useful for transient measurements stem from their inherent linearity and wide dynamic range.

Rogowski coil has been successful used for measure and extract high frequency PD signals in covered-conductor line [9]. In this work to follow, the performance of Rogowski coil will be tested to measure and extract high frequency surge transient traveled along the covered-conductor and uncovered overhead lines due to different fault conditions. Recently, normal current transformer (CT) is used to measure this signal. However, the responses of conventional current transformers (CTs) at high frequencies are not flat. Rogowski coil can be used as an alternative.

2 ROGOWSKI COIL AS A FAULT SENSOR

A Rogowski coil is basically a low-noise, toroidal winding on a non-magnetic core (generally air-cored), placed around the conductor to be measured, a fact that makes them lighter and smaller than iron-core devices.

To prevent the influence of nearby conductors carrying high currents, the Rogowski coil is designed with two wire loops connected in electrically opposite directions [4]. This will cancel all electromagnetic fields coming from outside the coil loop. The first loop is made-up of turns of the coil, and the other loop can be formed by returning the wire through the centre of the winding as shown in Figure 1(a), where d_1, d_2, and d_{rc} are internal, external, and net diameters of the Rogowski coil, respectively. The coil is effectively a mutual inductor coupled to the conductor being measured and the output from the winding is an electromotive force proportional to the rate of change of current in the conductor. This voltage is proportional to the current even when measuring complex waveforms, so these transducers are good for measuring complex transients and for applications where they can accurately measure asymmetrical current flows.

The self inductance of the coil is fixed, and its mutual inductance with the HV test circuit varies to some extent (or slightly) depending on the position of the coil in relation to the conductor. But once the coil is clamped and held stationary, the mutual inductance remains constant. Usually the coil is not loaded and the voltage appearing across it is used as PD/fault transient measurement signal. Under this condition, the coil voltage is directly proportional the derivative of the current in the conductor. Owing to the small value of the mutual inductance, the sensor acts as a high-pass filter, therefore, it attenuates the power frequency component of the current in the conductor and minimizes electromagnetic interference at lower frequencies. The coils are designed to give a high degree of rejection to external magnetic fields, e.g., from nearby conductors. The coils are wound either on a flexible former, which can then be conveniently wrapped around the conductor to be measured or wound on a rigid former, which is less convenient but more accurate. Both of these transducer types exhibit a wide dynamic range, so the same Rogowski coil can often be used to measure currents from mA to kA. They also exhibit wideband characteristics, typically useful up to hundreds of MHz, too. All these are gained with low phase error and without the danger of open circuited secondary (as could happen in case of CT). A typical mutual inductance of a standard flexible Rogowski coil (used in this research work) is up to 200-300 nH and its resonant frequency lies in the high frequency spectrum at 29 MHz [5, 6].

3 SIMULATION STUDY

A. MV Network and Rogowski Coil Modeling

The Rogowski configuration and its equivalent simulated circuit is shown in Figure 1 where the number of turns is 1900 turns with inner diameter 101 mm and outer diameter 109 mm. The corresponding equivalent circuit is R_l = 63 Ω, L_l = 0.191 mH and C_l = 51.6 pF with terminating impedance Z_{out} = 3 kΩ. Different types of fault are created in section F-G in feeder EFGH. Rogowski coils E, F, and G is selected to evaluate it performance in order to detect different types of fault conditions.

MV network distribution lines with 4-feeder is shown in Figure 2 where this network earth fault current is compensated. The overhead lines feeder is energized by AC sinusoidal waveforms via 110/20 kV, delta/star transformer. The covered and non-covered overhead lines are represented using JMarti frequency model where their configurations are shown in Figure 3. High frequency transformer model presented in [10-11] is added to the power model for accurately representing of electromagnetic transients of 21/0.42 kV load transformers. The parameters of this high frequency model are summarized in Figure 4. The effect of the high frequency added model is found that reflection signal from the MV-LV transformers path to the network is reduced. Rogowski coils model presented in [9] is used and allocated on the lines at distance 4 km between others.

The compensated MV network and the corresponding measuring devices are simulated using the EMTP-ATP simulation environment. ATPDraw is used as a pre-processor [7-8]. Therefore, the performance of the Rogowski coil is evaluated concerning different fault scenarios such as resistance, leaning trees and arcing faults. The dynamic modeling of these faults is discussed in the following subsections. The evaluation is carried out with generated different fault types, different fault resistances and different fault inception angles considering locations of Rogowski coils shown in Figure 2. These fault conditions are simulated considering fault distance 1.5 km from the Rogowski coil F on the tested MV network.

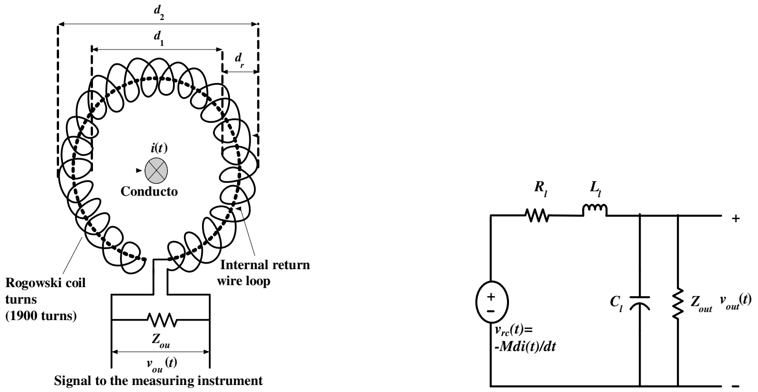

(a) (b)

Figure 1: The Rogowski coil. (a) Geometry and construction. (b) Equivalent circuit (lumped parameters model).

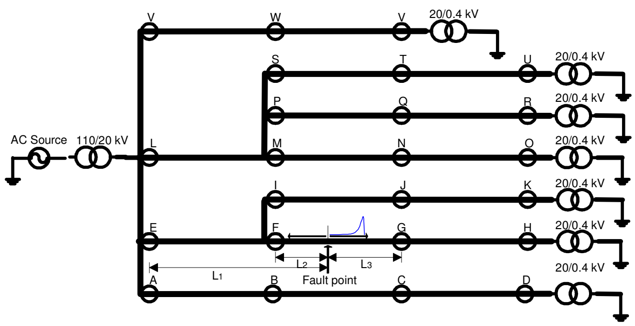

Figure 2: Simulated system for 78 km distribution network. O the Rogowski coil location.

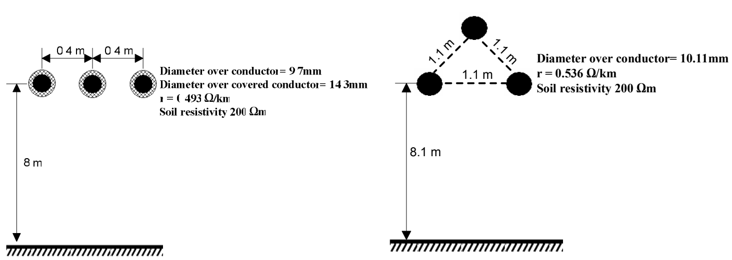

(a) (b)

Figure 3: The feeder configuration. (a) Covered conductor over head line, (b) Uncovered conductore overhead line.

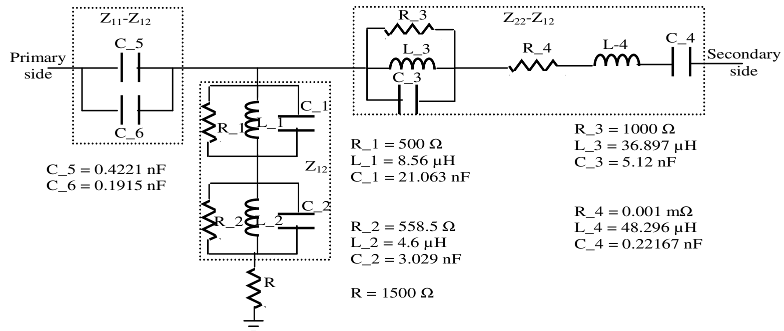

Figure 4: High Frequency Model of MV/LV Transformer and its parameters [10].

B. Model of fault due to leaning tree

An experiment was performed to measure the characteristics of faults due to leaning trees occurring in a 20 kV distribution network [12]. This fault type is modeled using two series parts: a dynamic arc model and a high resistance. For the considered case study, the resistance is equal to 140 kΩ and the arc is modeled using thermal equilibrium that is adapted as [12]:

$$\frac{dg}{dt} = \frac{1}{\tau}(G - g) \tag{1}$$

$$G = \frac{|i|}{U_{arc}} \tag{2}$$

$$\tau = Ae^{Bg} \tag{3}$$

where g is the time-varying arc conductance, G is the stationary arc conductance, $|i|$ is the absolute value of the arc current, U_{arc} is a constant arc voltage parameter, τ is the arc time constant and A and B are constants. In [12], the parameters U_{arc}, A and B were found to be 2520V, 5.6E-7 and 395917, respectively. Considering the conductance at each zero crossing, the dielectric is represented by a variable resistance until the instant of reignition. It is represented using a ramp function of 0.5 MΩ/*ms* for a period of 1 *ms* after the zero-crossing and then 4 MΩ/ms until the reignition instant.

C. Model of arcing fault

A dynamic model of arcing fault in distrbiution networks was presented by Kizilcay et. al. in [13] where the dynamic arc equations (1) and (2) are the same with concerning a suitable form of the arc time constatnt as in [13]:

$$\tau = \tau_o\left(\frac{l}{l_o}\right)^{\alpha} \tag{4}$$

The arc time constant τ is function of the arc length l where τ_o is the initial arc time constant, l_o is the initial arc length and α is a coefficient of negative value. Towards implementing this arcing fault model, dynamic equations (1), (2) and (4) are solved and interacted with the network. U_{arc} is is in the form:

$$U_{arc} = (u_o + r|i|)l \qquad (3)$$

$$u_o = 900 + \frac{400}{l} \quad \text{and} \quad r = 0.04 + \frac{0.008}{l} \qquad (4)$$

where r is the resistive component per arc length, u_o is constant voltage per arc length. The value of the model parameters are: τ_o =0.25 ms, α =-0.4 and l_o =0.20 m. This arcing fault model is implemented considering the effect of arc eleongation with rate of change equal to 10.5 m/s.

Regarding the EMTP program, a major breakthrough was the 1976 addition of Transients Analysis of Control Systems (TACS) to EMTP [14]. For the first time, power system transients and control systems could be modeled simultaneously in order to study their dynamic interaction. “Sensors” pick up signals from the power systems (often called the Network) for input to the control system (often called TACS). Commands are forwarded from the control system to the power system. Considering the bilateral interaction between the EMTP power network and the TACS field, the arcing equations and their corresponding parameters are implemented using the universal arc representation as addressed in [15]. The aforementioned MV network and the fault modeling are combined in a single arrangement to describe the network behavior, accordingly.

Figure 5 shows the ATPDraw circuit declaring the power feeders, the high frequency and saturable models of the load transformers, Rogowski coil model and the univeral arc representation of the arc. The sampling frequencies are considered 100 MHz for resistance fault cases and 1 MHz for tree-leaning and arcing fault cases.

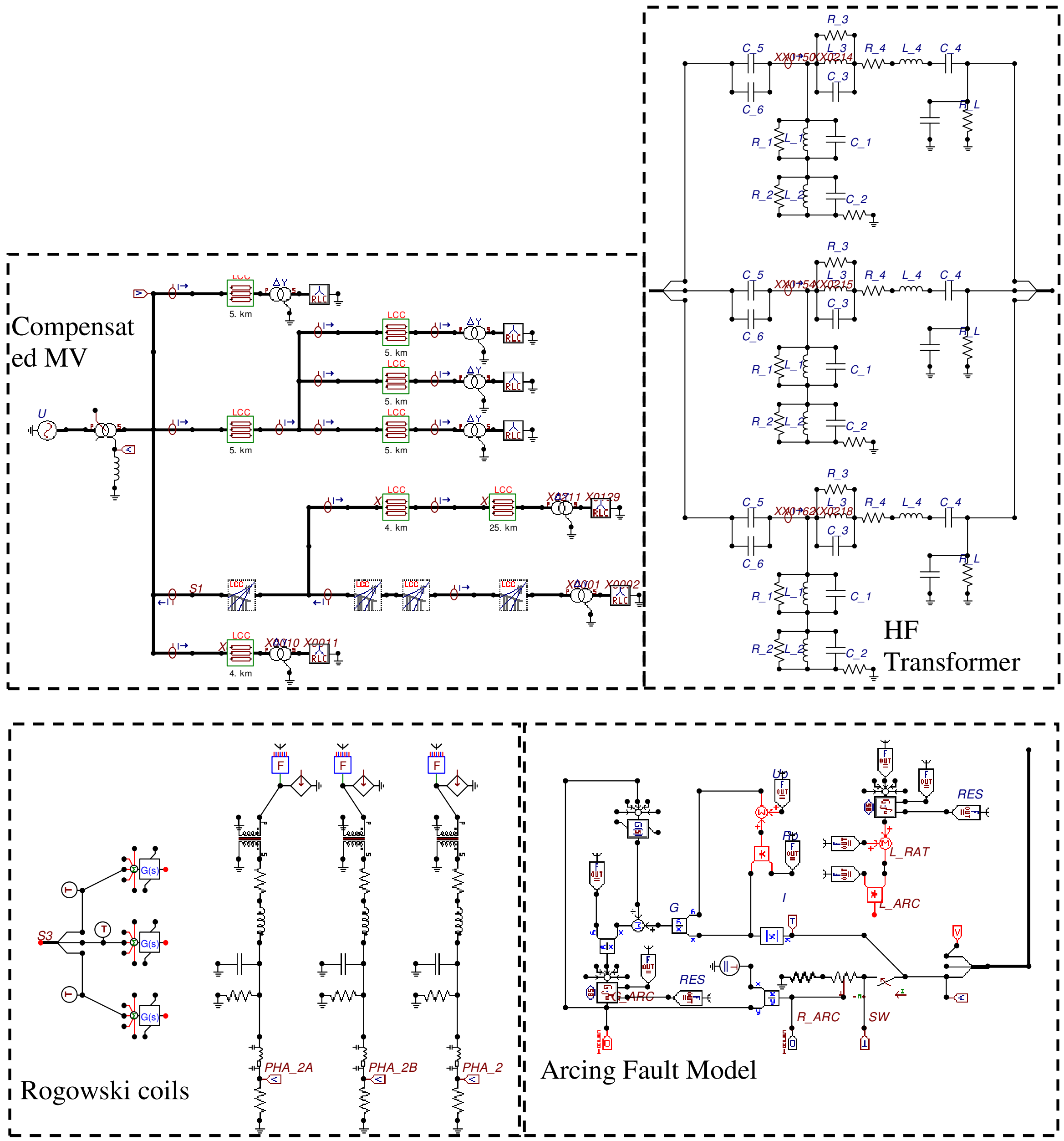

Figure 5: ATPDraw circuit.

4 Performance Evaluation of Rogowski coil

A. The performance considering resistance fault cases

Considering earth fault in phase C at the fault point in the network shown in Figure 2 where this network is with covered conductor feeders, Figure 6 shows the measurements of Rogowski coils installed at E, F and G nodes. From the waveforms shown in Figure 6, the fault surges can be measured using the Rogowski coils with sufficient large voltage range of 5 to 15 V.

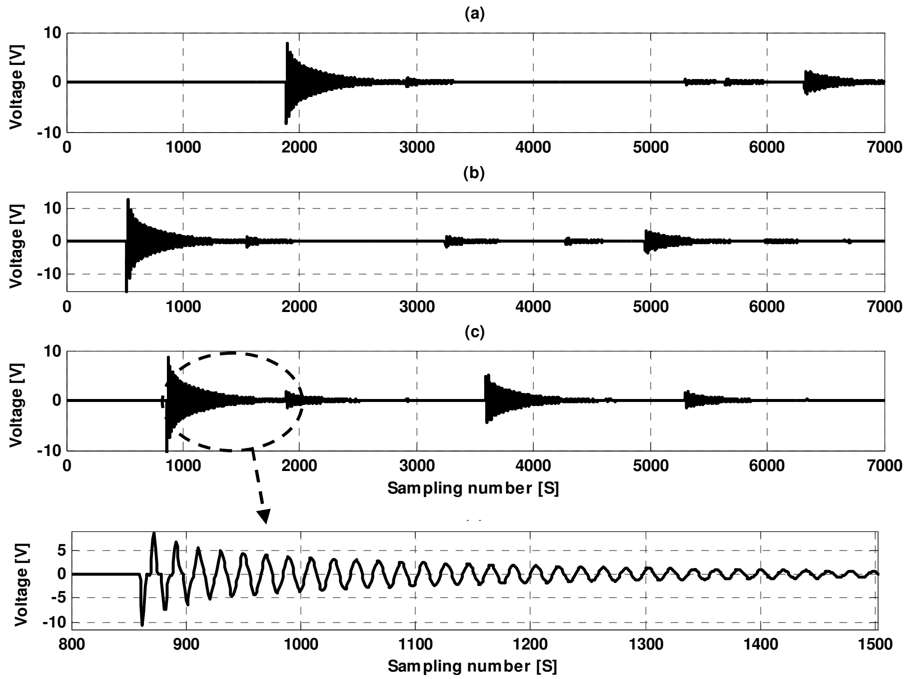

Figure 6: Rogowski coil response for solidly earth fault of phase C, (a) RC_E, (b) RC_F, (c) RC_G.

For resistivity faults, the value of fault resistance is changed in the arnge 1 mΩ to 3 MΩ. Table I shows the corresponding performance of high frequency Rogowski coils for single phase to ground fault. It is found that the maximum value for Rogowski coil response on phase C is higher than the other phases. This is due to the fault occurs on phase C. The corresponding response of high frequency Rogowski coils on phase A and B is due to the effect of electromagnetic and static couplings of the overhead feeder phases. Also from Table I, increasing the fault resistance reduces the measured maximum voltage measured by Rogowski coil. This is proportional to the level of transient traveling surges produced by the fault. High resistance fault will produce less value of traveling waves compare to low resistance fault. The measured voltage is extremly reduced for fault resistances of MΩ where at such fault resistances the measured voltages are low comparing with the voltages measured with PD sources. The table results confirm the Rogowski coil suitability to extract the earth fault surges that are extremly dificult to find when the network is compensated network.

TABLE I. THE PERFORMANCE EVALUATION OF ROGOWSKI COIL CONSIDERING DIFFERENT RESISTANCE FOR SINGLE PHASE TO GROUND FAULT RESISTIVITY

R_f (Ω)	$V_{RC1,peak}$ (V)			$V_{RC2,peak}$ (V)			$V_{RC3,peak}$ (V)		
	Phase A	Phase B	Phase C	Phase A	Phase B	Phase C	Phase A	Phase B	Phase C
1e-3	**4.3601**	**4.7443**	**8.4431**	**7.0758**	**6.8571**	**15.1191**	**4.9712**	**5.6389**	**10.7987**
1	**4.3413**	**4.7242**	**8.4074**	**7.0452**	**6.8271**	**15.0535**	**4.9499**	**5.6150**	**10.7527**
1000	**0.8177**	**0.9017**	**1.6074**	**1.3226**	**1.3113**	**2.8182**	**0.9336**	**1.0736**	**2.0429**
10k	**0.0984**	**0.1088**	**0.1940**	**0.1590**	**0.1586**	**0.3385**	**0.1123**	**0.1295**	**0.2462**
100k	**0.0100**	**0.0111**	**0.0198**	**0.0162**	**0.0162**	**0.0345**	**0.0115**	**0.0132**	**0.0251**
500k	**0.0020**	**0.0022**	**0.0040**	**0.0032**	**0.0032**	**0.0069**	**0.0023**	**0.0027**	**0.0050**
1M	**0.0010**	**0.0011**	**0.0020**	**0.0016**	**0.0016**	**0.0035**	**0.0011**	**0.0013**	**0.0025**
2M	**5.031e-4**	**5.510e-4**	**9.870e-4**	**8.123e-4**	**8.107e-4**	**0.0017**	**5.740e-4**	**6.63e-4**	**0.0013**
3M	**3.355e-4**	**3.656e-4**	**6.563e-4**	**5.414e-4**	**5.402e-4**	**0.0012**	**3.825e-4**	**4.43e-4**	**8.39e-4**

In Table II, the response of high frequency Rogowski coils at point E, F, and G is showing up when phase faults occured between phases B and C at the same fault location in Figure 2. The maximum value of Rogowski coil response on phase B and C is clearly higher than phase A for each resistance fault. Comparing the measured votages due to earth faults (Table I) and due to phase faults (Table II), the voltages due to phase faults are higher than earth faults where the sequence networks can help to interpret such a comparitive performance. Table III sumarizes Rogowski coils response at point E,F, and G for three-phase fault type.

TABLE II. THE PERFORMANCE EVALUATION OF ROGOWSKI COIL CONSIDERING DIFFERENT RESISTANCE FOR PHASE (B) TO PHASE (C) FAULT RESISTIVITY

R_f (Ω)	$V_{RC1,peak}$ (V)			$V_{RC2,peak}$ (V)			$V_{RC3,peak}$ (V)		
	Phase A	Phase B	Phase C	Phase A	Phase B	Phase C	Phase A	Phase B	Phase C
1e-3	**1.967**	**24.322**	**22.528**	**1.729**	**37.470**	**37.812**	**1.762**	**29.210**	**28.109**
1	**1.960**	**24.233**	**22.446**	**0.172**	**37.329**	**37.670**	**1.756**	**29.104**	**28.007**
1000	**0.425**	**5.226**	**4.847**	**0.377**	**7.955**	**7.917**	**0.380**	**6.290**	**6.022**
10k	**0.053**	**0.648**	**0.601**	**0.047**	**0.990**	**0.975**	**0.047**	**0.780**	**0.746**
100k	**0.005**	**0.066**	**0.062**	**0.005**	**0.102**	**0.1000**	**0.005**	**0.080**	**0.076**
500k	**0.001**	**0.013**	**0.012**	**0.001**	**0.020**	**0.020**	**0.001**	**0.016**	**0.015**
1M	**0.00054**	**0.0066**	**0.0062**	**0.00048**	**0.0102**	**0.01**	**0.00048**	**0.008**	**0.0077**
2M	**0.00027**	**0.0033**	**0.0031**	**0.00024**	**0.0051**	**0.0050**	**0.00024**	**0.004**	**0.0038**
3M	**0.00018**	**0.0022**	**0.0021**	**0.00016**	**0.0034**	**0.0033**	**0.00016**	**0.0027**	**0.0026**

TABLE III. THE PERFORMANCE EVALUATION OF ROGOWSKI COIL CONSIDERING DIFFERENT RESISTANCE FOR THREE PHASE FAULT RESISTIVITY

R_f (Ω)	$V_{RC1,peak}$ (V)			$V_{RC2,peak}$ (V)			$V_{RC3,peak}$ (V)		
	Phase A	Phase B	Phase C	Phase A	Phase B	Phase C	Phase A	Phase B	Phase C
1e-3	**5.7643**	**26.9128**	**21.1485**	**9.8934**	**42.5986**	**34.4929**	**5.7088**	**32.5811**	**26.8723**
1	**5.6965**	**26.6970**	**21.0005**	**9.7713**	**42.2443**	**34.2642**	**5.6355**	**32.3184**	**26.6830**
1000	**0.3127**	**2.9526**	**2.6923**	**0.3610**	**4.53**	**4.4082**	**0.2163**	**3.5578**	**3.3618**
10k	**0.0286**	**0.3275**	**0.3051**	**0.0270**	**0.5009**	**0.4953**	**0.0245**	**0.3945**	**0.3790**
100k	**0.0028**	**0.0331**	**0.0309**	**0.0026**	**0.0506**	**0.0501**	**0.0026**	**0.0399**	**0.0384**
500k	**0.00056**	**0.0066**	**0.0062**	**0.00051**	**0.0101**	**0.0100**	**0.00052**	**0.0080**	**0.0077**
1M	**0.00028**	**0.0033**	**0.0031**	**0.00025**	**0.0051**	**0.0050**	**0.00026**	**0.0040**	**0.0038**
2M	**0.00014**	**0.0017**	**0.0015**	**0.00013**	**0.0025**	**0.0025**	**0.00013**	**0.002**	**0.0019**
3M	**0.00009**	**0.00008**	**0.00008**	**0.00008**	**0.0017**	**0.0017**	**0.00008**	**0.0013**	**0.0013**

In the analysis of the inception angle influence, cases corresponding to single phase to ground, with fault resistance is 1 mΩ and inception angle varied from 0 to 90°. The results are shown in Table IV. The Rogowski coils response is affected by the limitation of zero voltage point on waves faults which is regarded as a major problem for pure traveling wave techniques, but it is still adequate to give the correct response.

TABLE IV. THE PERFORMANCE EVALUATION OF ROGOWSKI COIL CONSIDERING DIFFERENT INCEPTION ANGLE FOR SINGLE PHASE FAULT (R=0.001 Ω)

Inception angle degree	$V_{RC1,peak}$ (V)			$V_{RC2,peak}$ (V)			$V_{RC3,peak}$ (V)		
	Phase A	Phase B	Phase C	Phase A	Phase B	Phase C	Phase A	Phase B	Phase C
0	**8.6386e-004**	**9.1806e-004**	**0.0017**	**0.0014**	**0.0013**	**0.0030**	**9.7204e-004**	**0.0011**	**0.0021**
10	**3.8027**	**4.1377**	**7.3636**	**6.1711**	**5.9804**	**13.1860**	**4.3356**	**4.9179**	**9.4180**
30	**2.4543**	**2.6705**	**4.7526**	**3.9829**	**3.8598**	**8.5104**	**2.7983**	**3.1741**	**6.0785**
45	**1.2382**	**1.3474**	**2.3978**	**2.0095**	**1.9474**	**4.2937**	**1.4118**	**1.6014**	**3.0668**
60	**0.0622**	**0.0676**	**0.1203**	**0.1008**	**0.0977**	**0.2155**	**0.0708**	**0.0804**	**0.1539**
90	**2.5619**	**2.7876**	**4.9610**	**4.1575**	**4.0290**	**8.8836**	**2.9210**	**3.3133**	**6.3450**

B. The performance considering leaning-tree and arcing fault cases

The faulty feeder is replaced by simulated uncovered conductor in order to take the leaning-tree and arcing fault modeling into considerations. Figure 7 and 8, show the Rogowski coil performance to detect high frequency transient signal due to leaning of tree and intermittent fault respectively. It is shown the capability of Rogowski coil to measure these high impedance faults. The measurements of leaning-tree and arcing fault are made at zero crossing degree very difficult to measure it using other measuring transducer. Although the measured signals by Rogowski coils in these fault cases is small than most of PD cases, the possibility to locate the fault source location still have.

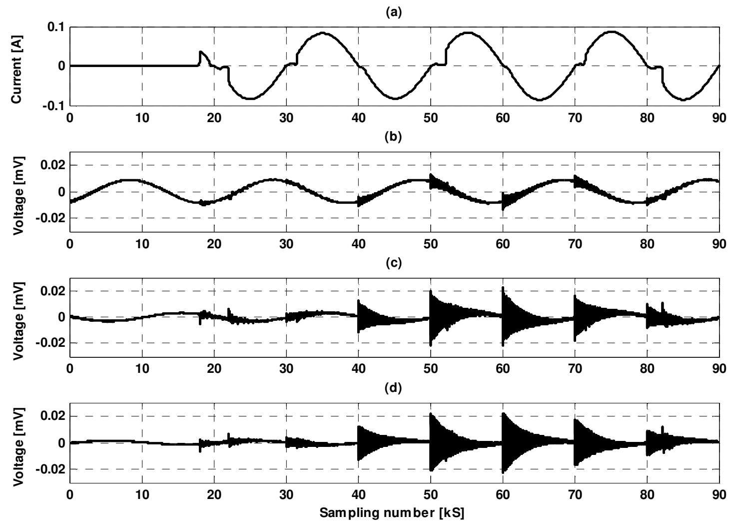

Figure 7: Rogowski coils response for high impedance fault due to leaning tree, (a) leaning tree current fault, (b) RC_E, (c) RC_F, and (d) RC_G.

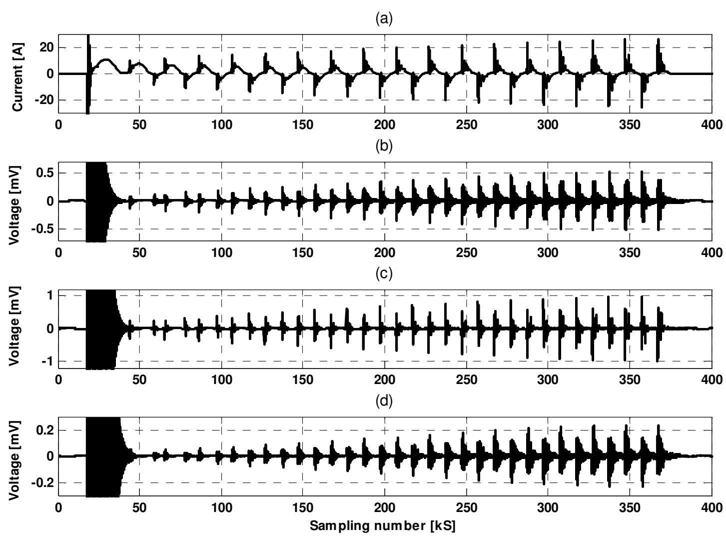

Figure 8: Rogowski coils response for intermittent fault, (a) Intermittent phase current (b) RC_E, (c) RC_F, and (d) RC_G.

5 CONCLUSIONS

Capability of the high frequency Rogowski coil to measure and extract high frequency transient fault due varied fault conditions has been proved. Different value of fault resistance and inception angle due to earth faults is tested on the MV distribution networks in order to investigate the performance of Rogowski coil. High impedance fault due to leaning tree and intermittent fault have been modeled where thier corresponding fault traveling surges have been measured and extracted by Rogowski coil. Sensitivity of each Rogowski coil and the surge arrival time have been found proportional to the distance where the fault surge travelled upto the measuring point. In a work to follow, measured signal by Rogowski coil will be used to locate the fault source location by implementing multi-end correlation techniques.

7 REFERENCES

[1]G. Xiaohua, L. Jingsheng, Z. Mingjun, and Y. Miaoyuan, “Improved Performance Rogowski Coils for Power System ” Transmission and Distribution Conference and Exposition, IEEE Power Engineering Society, Wuhan, China, Vol. 1, pp 371-374, 2003.

[2]D. A. Ward and J. L. T. Exon, "Experience with using Rogowski Coils for Transient Measurements" Pulsed Power Technology, IEE Colloquium, pp. 61-64, 1992.

[3]Z. Mingjuan, D. J. Perreault, and V. Caliskan, “Design and Evaluation of an Active Ripple Filter with Rogowski Coil Current Sensing”,IEEE 30th Annual Power Electronics Specialists Conference, Vol. 2, pp.874-880, 1999.

[4]L. A. Kojovic, “Rogowski Coil Transient Performance and ATP Simulations for Applications in Protective Relaying”, International Conference on Power Systems Transients (IPST’05), Montreal, Canada, Paper No. 010, 2005.

[5]D. A. Ward and J. La T. Exon, “Using Rogowski Coils for Transient Current Measurement”, Engineering Science and Education J., Vol. 2, pp. 105-113, 1993.

[6]L. A. Kojovic, “Rogowski Coil Suit Relay Protection and Measurement of Power Systems”, IEEE Computer Applications in Power, Vol. 10, No.3, pp.47-52, 1998.

[7]ATP – EMTP Rule Book, Canadian – American EMTP User Group, 1997.

[8]ATPDraw Version 3, User Manual, TR A4389, EFI, Norway, 1996.

[9]G. M. Hashmi, M. Lehtonen, and M. Nordman, “Modeling and Experimental Verification of On-line PD Detection in MV Covered-conductor Overhead Networks,” IEEE Transaction on Dielectrics and Electrical Insulation, vol. 17, Issue 1, Feb. 2010, pp. 167-180.

[10] N. A. Sabiha and M. Lehtonen “Lightning Induced Overvoltages Transmitted over Distribution Transformer with MV Spark-Gap Operation, Part I: High Frequency Transformer Model with MV Spark-Gap”, accepted at IEEE Transactions on Power Delivery.

[11] N. A. Sabiha and M. Lehtonen “Combining High Frequency and Saturable models of Distribution Transformer for Lightning-Induced Overvoltage Superimposed on AC Voltage” European EMTP-ATP Conference, EEUG Meeting 2010, 16-18 August, 2010, Espoo, Finland.

[12] N. I. Elkalashy, M. Lehtonen, H. A. Darwish, M. A. Izzularab and A. I. Taalab "Modeling and Experimental Verification of High Impedance Arcing Fault in MV Networks" IEEE Trans. Dielectric and Electrical Insulation, vol. 14, no. 2, pp. 375-383, April 2007.

[13] M. Kizilcay and P. Seta "Digital Simulation of Fault Arcs in Medium-Voltage Distribution Networks" 15th Power Systems Computation Conference, PSCC, Liege, Belgium, 22-26 August 2005.

[14] R. Lasseter, K. Fehrle and B. Lee Electromagnetic Transient Program (EMTP), Workbook IV (TACS). El-4651, EPRI Research Project 2140-6, Palo Alto, CA 94303, June 1989.

[15] H. Darwish and N. Elkalashy “Universal Arc Representation Using EMTP,” *IEEE Trans. on Power Delivery*, Vol. 2, no. 2, pp 774-779, April 2005.